Biomaterials Science

PAPER

View Article Online
View Journal | View Issue

Cite this: *Biomater. Sci.*, 2015, **3**, 352

Surface modulation of complex stiffness *via* layer-by-layer assembly as a facile strategy for selective cell adhesion†

Hao Chang, He Zhang, Mi Hu, Xia-chao Chen, Ke-feng Ren,* Jin-lei Wang and Jian Ji*

Received 11th September 2014,
Accepted 15th November 2014

DOI: 10.1039/c4bm00321g

www.rsc.org/biomaterialsscience

In-stent restenosis and thrombosis are the main severe problems that occur after the percutaneous vascular intervention. The competition between endothelial cells (ECs) and smooth muscle cells (SMCs) plays a key role during these pathological changes. The regulation of this competition offers new opportunities to design biomaterials in the cardiovascular fields. Bioactive molecules have been typically employed to increase EC adhesion and thereafter to enhance EC competitiveness; however, this method is associated with limitations from the point of view of practical and industrial applications. Herein, we present an approach to enhance EC competitiveness over that of SMC through the selective EC adhesion, which is achieved by modulating a complex surface stiffness based on the technique of layer-by-layer (LbL) assembly. This complex stiffness can be achieved by regulating the thickness of multilayer films coordinating with a rigid underlying substrate. The selective cell adhesion is attributed to changes in the complex surface stiffness and a different intrinsic property between ECs and SMCs. This study provides a facile and broadly applicable approach for the purpose of the enhancement of EC competitiveness over that of SMC, which has great potential for the development of cell-based functional biomaterials in the cardiovascular field.

Introduction

Cardiovascular disease remains the leading cause of disability and mortality in modern societies.[1] Percutaneous coronary intervention has been extensively developed in the treatment of cardiovascular disease. However, it is always accompanied by in-stent restenosis (ISR) which is usually caused by injury to the endothelium and over proliferation and migration of smooth muscle cells (SMCs).[2,3] Drug-eluting stents (DESs), which act to inhibit SMC proliferation, play an important role in reducing restenosis.[4,5] However, it has been suggested that the anti-proliferative drugs in DESs also inhibit endothelial cell (EC) growth, resulting in delayed re-endothelialization and severe late in-stent thrombosis.[6–8] Competitions among cells operate pervasively in organisms.[9–11] For example, competition between tumor cells and normal cells exists in tumorigenesis and tumor metastasis.[12,13] The competition between ECs and SMCs plays a key role during pathological changes. The enhancement of EC competitiveness over that of SMC is of critical importance for the promotion of rapid-endothelialization and reducing the risk of restenosis.[14,15]

Although extremely challenging, the surface immobilization of bioactive molecules has been typically employed to enhance EC competitiveness by promoting EC adhesion, proliferation, migration or functions.[16–19] However, there are limitations to the use of bioactive molecules in practical and industrial applications. These limitations include the need for complex processes for surface modification, the unstable bioactivities, and the mounting of immune responses *in vivo*. The development of a facile approach without using bioactive molecules would be of great help in gaining a better understanding of EC–SMC competition and for exploring potential applications.

In addition to chemical cues, stiffness, as a key mechanical factor of the cellular microenvironment, is known to greatly impact cell behaviours including adhesion, migration and differentiation.[20–22] Mesenchymal stem cells, for instance, differentiate into ECs on soft matrices while they differentiate into SMCs on rigid matrices.[23] Interestingly, different types of cells respond differently to the stiffness of their matrices.[24–26] For example, cortical neurons can spread well on soft gel while astrocytes do not.[25] More interestingly, differing from chemical

Department of Polymer Science and Engineering Key Laboratory of Macromolecule Synthesis and Functionalization of the Ministry of Education, Zhejiang University, 310027 Hangzhou, P.R. China. E-mail: renkf@zju.edu.cn, jijian@zju.edu.cn

†Electronic supplementary information (ESI) available: Fig. S1–S5. See DOI: 10.1039/c4bm00321g

signals, which generally need a direct contact with the cells for triggering bioactivities, the mechanical signals can have an influence on the target cells up to hundreds of micrometers away.[27,28] Therefore, cells can sense rigid underlying substrates through a soft superficial layer, like the proverbial princess who feels a pea placed beneath soft mattresses.[29,30] When cells contact a thin and soft layer affixed to an underlying rigid substrate, the apparent surface stiffness that the cells sense is the result of the stiffness of both soft and rigid surfaces. This stiffness is called the complex stiffness.[29–32]

Herein, we present a pure stiffness-controlled surface for achieving selective EC adhesion. The surface stiffness is modulated by using the layer-by-layer (LbL) assembly technique, which is a simple, inexpensive and highly versatile method for fabricating nanostructured multilayered thin films, consisting of a variety of materials, through a multitude of intermolecular interactions.[33,34] This technique was introduced by the pioneering work of Decher *et al.*[35] and has been widely applied for surface modifications, particularly for regulating the surface stiffness.[36,37] The stiffness is generally regulated by chemical or photo cross-linking[38,39] as well as by changes in pH or ionic strength values.[40] In opposition to these methods, we construct a soft protamine sulfate (PrS)/DNA multilayer film *via* the LbL assembly technique and combine the underlying stiff substrate to control a complex surface stiffness. The extent to which an underlying stiff substrate could be felt through the superficial materials depends on the thickness of the PrS/DNA films. Both EC and SMC adhesion, either in separated culture or co-culture, are studied. The surface stiffness of the system (top multilayer films with different numbers of layers + underlying substrates) is then characterized. Finally, different underlying substrates are used to demonstrate the broad applicability of this approach for the purpose of selective cell adhesion.

Results and discussion

The fabrication of PrS/DNA multilayer films

The LbL assembled multilayer films were prepared by the alternate deposition of PrS and DNA on a glass substrate. The growth rates of the PrS/DNA multilayer film components had a nearly linear correlation (Fig. 1a and S1†), suggesting the successful fabrication of the multilayer films. The thickness of the PrS/DNA multilayer films with bilayer numbers of 4, 8, 12 and 24 (*i.e.*, 4b, 8b, 12b and 24b) in a liquid environment was calculated using Q-tools software as shown in Fig. 1b. The surface stiffness of the PrS/DNA multilayer films was measured using the method of nanoindentation. As shown in Fig. 2, the Young's moduli of the 4b, 8b, 12b, and 24b multilayer films were 40.043 ± 9.650, 1.096 ± 0.118, 0.695 ± 0.049, and 0.086 ± 0.025 MPa, respectively. Therefore, the results shown in Fig. 2 indicate that an increase in bilayer number leads to a decrease in surface stiffness. The surface stiffness measured using the nanoindentation method hereafter refers to the complex stiffness.

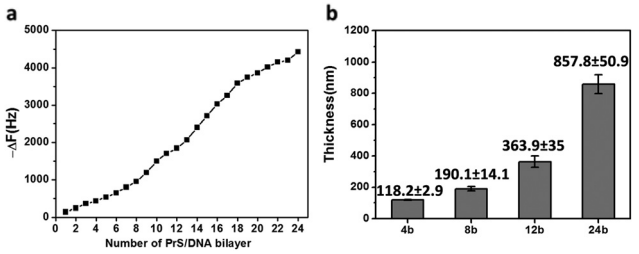

Fig. 1 The change of frequency shift as a function of the number of bilayers during the buildup of the PrS/DNA multilayer films determined using QCM-D in the liquid state (a). The thickness of the PrS/DNA multilayer films with bilayer numbers of 4, 8, 12 and 24 (4b, 8b, 12b and 24b, respectively) in a liquid environment obtained from QCM-D data (b).

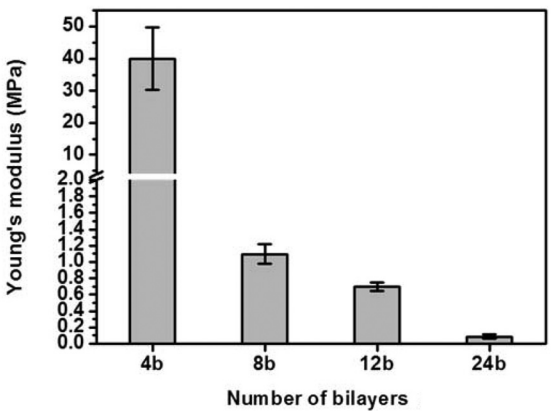

Fig. 2 Surface Young's modulus determined using a NanoIndenter for the PrS/DNA multilayer films with 4, 8, 12 and 24 bilayers (4b, 8b, 12b and 24b, respectively) on glass substrates. The indentation depth is 100 nm. $N = 3$ parallel samples per group. The data are representative of three independent experiments.

The adhesion of ECs and SMCs

ECs and SMCs were separately cultured on PrS/DNA multilayer films with bilayer numbers of 0, 4, 8, 12 and 24 (0b refers to the bare substrate). According to the data presented in Fig. 3a, c and d, both EC and SMC adhesion was found to decrease as the bilayer number increased. Interestingly, the decrease in the number of adherent cells with the increase in bilayer number was much faster for SMCs than for ECs. Almost no adherent SMCs could be found on the 12b multilayer films whereas ECs still adhered to the surface. This led to the hypothesis that selective EC/SMC adhesion could be achieved by varying the number of PrS/DNA bilayers in this multilayer film system. In order to test this hypothesis, cell adhesion experiments were then carried out in EC–SMC cocultures. Immunofluorescence was implemented for specific cell staining of ECs (by anti-vWF, red) and SMCs (by anti-calponin, green). Only in a contractile state can the SMCs express calponin. In this study, the 4 h adhesion was observed and the SMCs were still in the contractile state during this period. Therefore, almost all SMCs can express calponin in these coculture experiments. As seen in Fig. 3b, SMC adhesion was

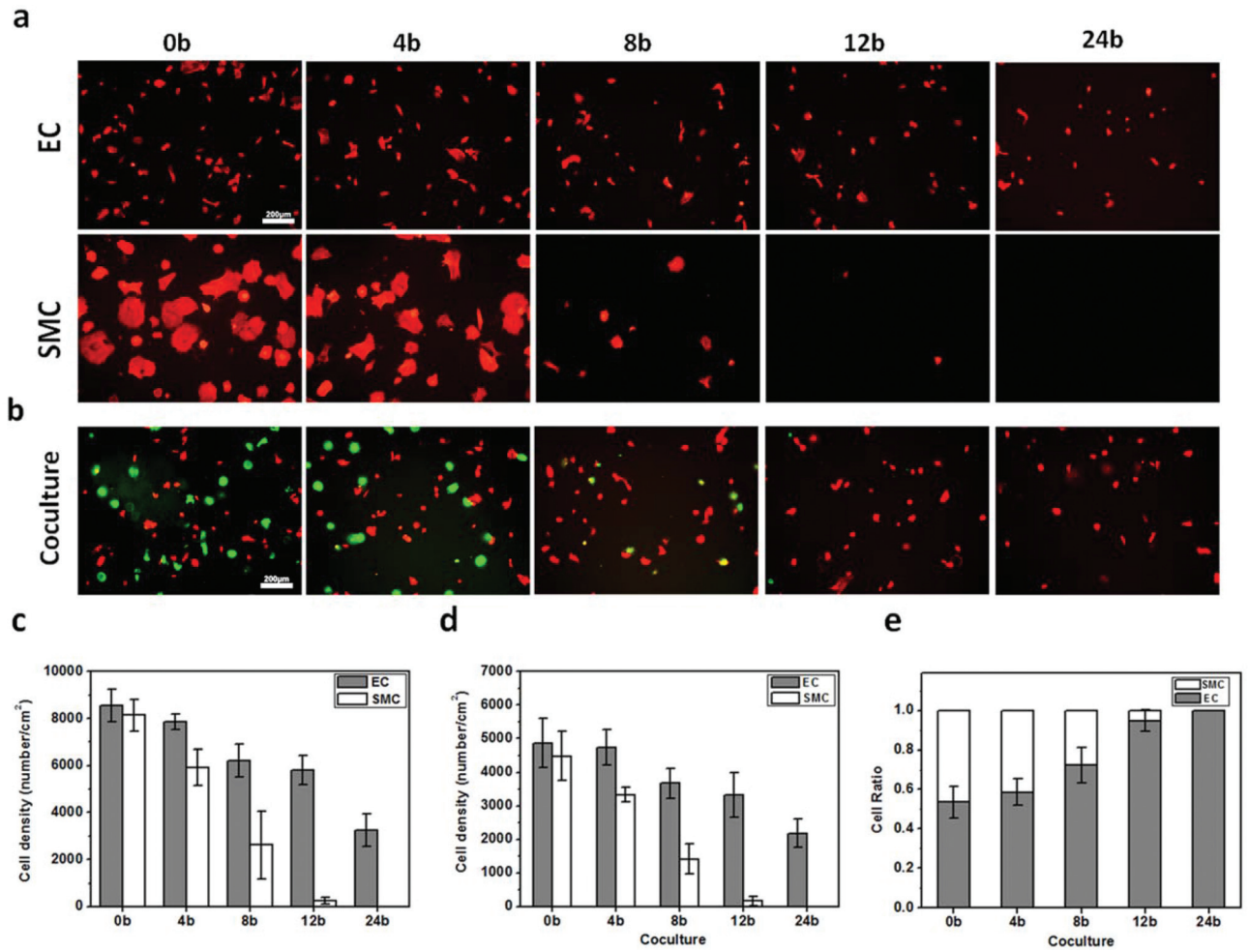

Fig. 3 The phenomenon of EC/SMC selective adhesion on PrS/DNA multilayer films with different bilayer numbers. Fluorescence microscopy images of ECs and SMCs cultured on the PrS/DNA multilayer films with 0, 4, 8, 12 and 24 bilayers (0b, 4b, 8b, 12b and 24b, respectively) fabricated on a glass substrate (cells were stained using F-actin, red) (a). Immunofluorescence images of ECs (stained using anti-vWf, red) and SMCs (stained using anti-calponin, green) in coculture on the PrS/DNA multilayer films with 0, 4, 8, 12 and 24 bilayers fabricated on a glass substrate (b). The density of adherent ECs and SMCs with the increasing number of bilayers (c). The density of adherent ECs and SMCs in coculture (d). The adherent cell ratio of EC : SMC in coculture (e). N = 5 parallel samples per group. The data are representative of three independent experiments. The scale bar is 200 μm.

nearly inhibited on the 12b multilayer films, but ECs were still adhering. Fig. 3e shows the ratio of adherent EC : SMC which was calculated from the percentage of cells that were ECs or SMCs occupying a whole image. It indicates a remarkable increase in selective EC adhesion efficiency with the increase in bilayer number. These results show that PrS/DNA multilayer films of different bilayer number, *i.e.*, thickness, can achieve regulation of EC/SMC competition due to varying cell adhesion.

The controlled surface stiffness leads to selective EC adhesion

It has been reported that chemical[41–43] and topographical factors[44,45] strongly influence cell adhesion and phenotype. When the topography of the PrS/DNA multilayer films was first characterized, it was found that all, regardless of the bilayer number, had flat surfaces that were not very rough (Fig. S2 and Table S1†). Although slight changes can be observed in both the morphology and roughness of the PrS/DNA multilayer films with increasing bilayer number, the influence of these differences on cell adhesion can be considered negligible because the values of roughness were within 2 nm.

To identify whether the chemistry of either PrS or DNA could have contributed to the selective EC/SMC adhesion, a different polyelectrolyte pair, poly(allylamine hydrochloride)/poly(sodium 4-styrenesulfonate) (PAH/PSS), was used to fabricate another multilayer film. The EC–SMC coculture experiments using PAH/PSS multilayer films also showed a successful selective cell adhesion (Fig. S3†). In this case, 48b was the best bilayer number for the selective cell adhesion, which could have resulted from using different polyelectrolytes and bilayer thickness. These data suggest that neither the chemistry nor topography of the PrS/DNA multilayer films was associated with the difference in EC *versus* SMC selective adhesion.

In addition to chemical and topographical cues, mechanical properties of the substrate play an important role during cell adhesion.[26,46] Tissue cells are generally anchorage dependent and are sensitive to the stiffness of the microenviron-

ment,[47] thus surface stiffness could greatly impact cell behaviors including cell-matrix adhesion.[48–50] We thus focused on whether differences in the surface stiffness of the PrS/DNA multilayer films with different bilayer numbers could account for the selective EC/SMC adhesion.

In this study, both the inherent stiffness of the multilayer film and the substrate contributed to a measurement of complex surface stiffness.[32] The mechanism of surface stiffness modulation is based on a fact that instruments can measure or cells can sense the stiffness of rigid objects with which they are not in direct contact.[29,30] The extent to which the underlying substrate stiffness can be detected depends on the thickness of the superficial compliant layer.[51] In this study, increasing the bilayer number, *i.e.*, increasing the multilayer film thickness (Fig. 1b), led to a decrease in the combined surface stiffness. In addition, it can also be said that decreasing the surface stiffness led to a decrease in the both number (Fig. 3c) and spreading areas (Fig. S4†) of adherent ECs and SMCs. The cells exhibited a similar phenomenon to what was previously reported; cells cannot spread well on low-stiffness surfaces.[36] Based on all the data, we conclude that the change in surface stiffness was the main factor accounting for the selective EC/SMC adhesion.

The intrinsic property differences between ECs and SMCs induce selective EC adhesion

Both EC and SMC adhesion decreased with the stiffness of the surface, and we were interested in investigating why these cell types responded differently. We observed changes in the cytoskeleton and focal adhesions (FAs) using fluorescence microscopy of cells stained for F-actin and vinculin. In SMCs, F-actin and FAs were diffuse, and the number of FAs and length of the FAs decreased with decreasing multilayer film stiffness to a greater degree than observed in ECs (Fig. 4 and 5). This suggests that SMCs might be more sensitive than ECs to surface stiffness. Generally speaking, cells adhere to substrates primarily through organized actin networks that associate with actomyosin to form contractile stress fibers.[52] Stress fibers terminate directly at FAs, where adhesion-related proteins such as integrins act as "hands to grip the surface".[21] These stress fibers can generate the intracellular tension force during cell adhesion and spreading. In order to maintain cell adhesion and spreading, the matrix should be stiff enough to provide a sufficient traction field at the interface between each cell and its matrix to balance the intracellular tension force.[52–54] The tension force determines the cell stiffness[54,55] and SMCs have been reported to be much stiffer than ECs.[56–58] Therefore, SMCs have a higher internal tension force than ECs, and a relatively soft surface would not be sufficient to balance the internal tension force of SMCs for supporting SMC adhesion and spreading. The stiffness-mediated selective cell adhesion observed here might therefore originate from the innate differences of ECs and SMCs, such as intracellular tension and cell stiffness.

To provide further insights into selective cell adhesion, the cells were treated with Y27632, a Rho-kinase inhibitor.[59,60] After treatment, the SMC adhesion on the 12b multilayer films was significantly enhanced, and the ratio of adherent SMCs to

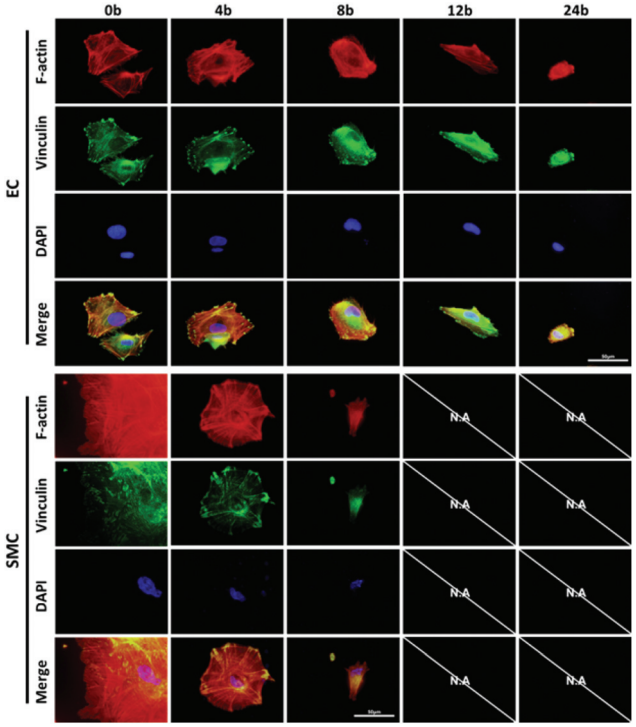

Fig. 4 Fluorescence microscopy images of ECs and SMCs stained for F-actin (red) and vinculin (green) and with DAPI (blue) after 4 h of adhesion on PrS/DNA multilayer films with 0, 4, 8, 12 and 24 bilayers (0b, 4b, 8b, 12b and 24b, respectively) fabricated on a glass substrate. The scale bar is 50 μm.

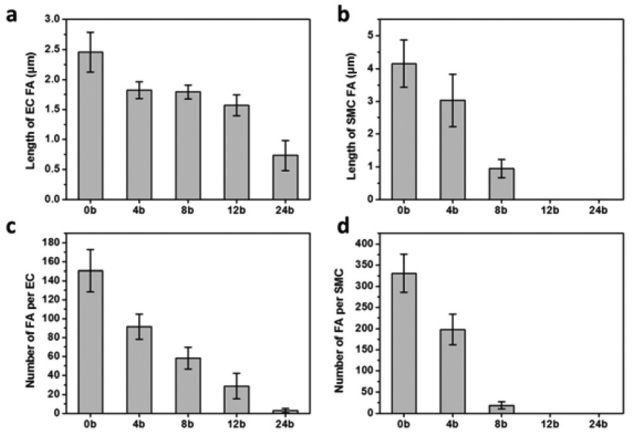

Fig. 5 Statistics data for ECs and SMCs stained for F-actin (red) and vinculin (green) after 4 h of adhesion on PrS/DNA multilayer films with 0, 4, 8, 12 and 24 bilayers (0b, 4b, 8b, 12b and 24b, respectively) fabricated on a glass substrate. The average length of the focal adhesions of ECs (a) and SMCs (b). The number of focal adhesions per EC (c) and SMC (d). $N = 5$ parallel samples per group. The data are representative of three independent experiments.

ECs was greatly increased, leading to the disappearance of the EC/SMC selection difference (Fig. 6). The inhibitor, Y27632, induces the disassembly of stress fibers, which results in relaxation and loss of contractile tension within the cells.[59–61] Obviously, the drug decreased the intracellular tension of

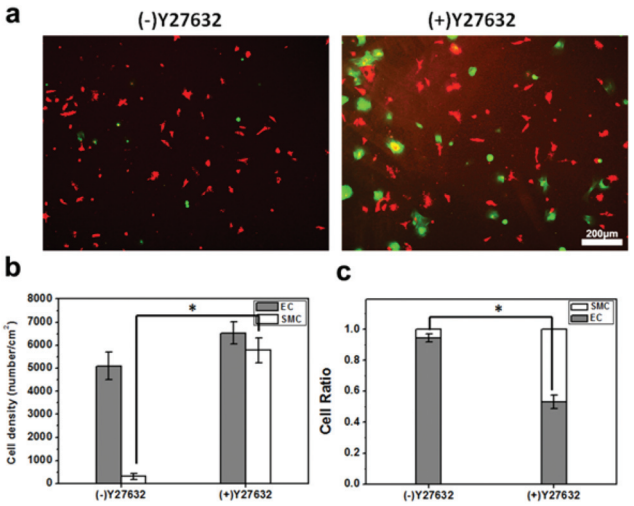

Fig. 6 The coculture of ECs (stained by anti-vWf, red) and SMCs (stained by anti-calponin, green) with or without the treatment of Rho-kinase inhibitor Y27632 after 4 h of adhesion on the 12b PrS/DNA multilayer films. Immunofluorescence images (a). The cell density of EC and SMC in coculture (b). The adherent cell ratio of EC : SMC in coculture (c). N = 5 parallel samples per group. The data are representative of three independent experiments, mean ± SD, *p < 0.05 compared with the group without Y27632 treatment. The scale bar is 200 μm.

SMCs, which decreased the sensitivity of the SMCs to the mechanical properties of the microenvironment. The data thus confirm a relationship between intracellular tension and selective EC/SMC adhesion. We believe that such mechanisms of selective cell adhesion could also be expanded to other kinds of cell pairs with inherently different properties, such as normal/cancer cells.[62]

The selective EC adhesion on multilayer films fabricated on various substrates

We next employed two widely used biomedical implant materials, polyethylene terephthalate (PET)[63] and stainless steel (SS),[64] as underlying substrates instead of the glass that was used in the other experiments. The coculture results showed that the EC selection properties on the 12b PrS/DNA multilayer films (Fig. 7, S5e and d†) were identical with those observed on the glass substrates. Actually, PET, SS and glass had multilayer film stiffness values at the magnitude of GPa.[65,66] They could thus be seen as infinitely stiff materials compared with the PrS/DNA multilayer film. In this case, PET, SS and glass substrates made the same contribution to the complex surface stiffness. Therefore, the selective EC adhesion appeared on the 12b PrS/DNA multilayer film regardless of the substrate that was used. However, it would be very interesting to investigate a very soft underlying substrate, such as poly-

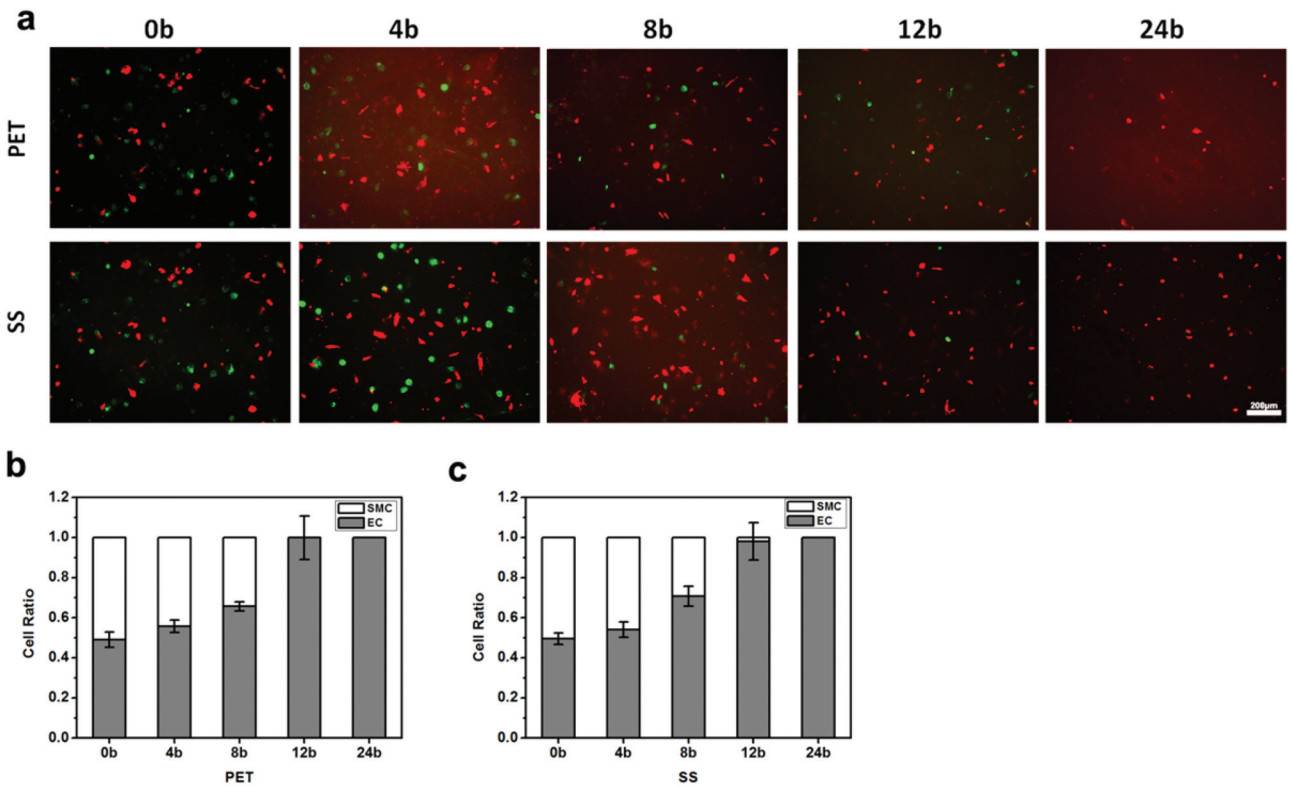

Fig. 7 Selective EC adhesion on the PrS/DNA multilayer films with 0, 4, 8, 12 and 24 bilayers (0b, 4b, 8b, 12b and 24b, respectively) fabricated on PET and SS substrates. Immunofluorescence images of ECs (stained using anti-vWf, red) and SMCs (stained using anti-calponin, green) in coculture (a). The cell ratio of EC : SMC in coculture when PET (b) and SS (c) were used as substrates. N = 5 parallel samples per group. The data are representative of three independent experiments. The scale bar is 200 μm.

dimethylsiloxane (PDMS), where the Young's modulus can be easily tuned by altering the cross-linking agent to base polymer stoichiometry.[67,68] Three ratios of crosslinker to PDMS elastomer base were used: 0.25 : 10, 0.5 : 10 and 1 : 10, resulting in materials with a stiffness of 0.798 ± 0.039, 1.138 ± 0.191 and 3.249 ± 0.291 MPa, respectively, as shown in Table 1.

Table 1 Surface Young's modulus (MPa), determined using a Nano-Indenter, for the $(PrS/DNA)_n$ multilayer films deposited on 0.25 : 10 PDMS, 0.5 : 10 PDMS and 1 : 10 PDMS substrates[a,b]

Bilayer number	1 : 10 PDMS	0.5 : 10 PDMS	0.25 : 10 PDMS
0b	3.249 ± 0.291	1.138 ± 0.191	0.798 ± 0.038
4b	2.905 ± 0.204	1.098 ± 0.116	0.614 ± 0.078*
8b	0.966 ± 0.126	0.682 ± 0.056*	n/a
12b	0.621 ± 0.056*	n/a	n/a

[a] $N = 3$ parallel samples per group. [b] *There is no significant difference in Young's modulus of surfaces of PrS/DNA multilayer films with 4b on 0.25 : 10 PDMS, 8b on 0.5 : 10 PDMS, 12b on 1 : 10 PDMS and 12b on glass substrates.

Interestingly, after being coated with the PrS/DNA multilayer films, the selective EC adhesion was achieved on 4b multilayer films for 0.25 : 10 PDMS, 8b for 0.5 : 10 PDMS and 12b for 1 : 10 PDMS, respectively (Fig. 8 and S5a–c†). The stiffness of the surfaces with cell selection properties were then measured, and they all had a value ~0.6 MPa, as shown in Table 1. These values are very close to the stiffness of the 12b PrS/DNA multilayer films on glass (0.695 MPa). The softer substrates (0.25 : 10 PDMS or 0.5 : 10 PDMS) require thinner multilayer films to reach the stiffness needed to achieve selective EC adhesion than the other tested surfaces (1 : 10 PDMS, PET, SS or glass). These data confirmed the relationship between complex surface stiffness and selective EC adhesion.

ECs and SMCs are two kinds of important cells involved in the establishment of the homogeneous blood vessel domains.[69,70] ECs and SMCs have their own competitiveness to restrict mutually and maintain the relative balance. Regulation of the competition between ECs and SMCs plays an important role in the cardiovascular system. Particularly, the promotion of EC adhesion over SMC adhesion is of significant

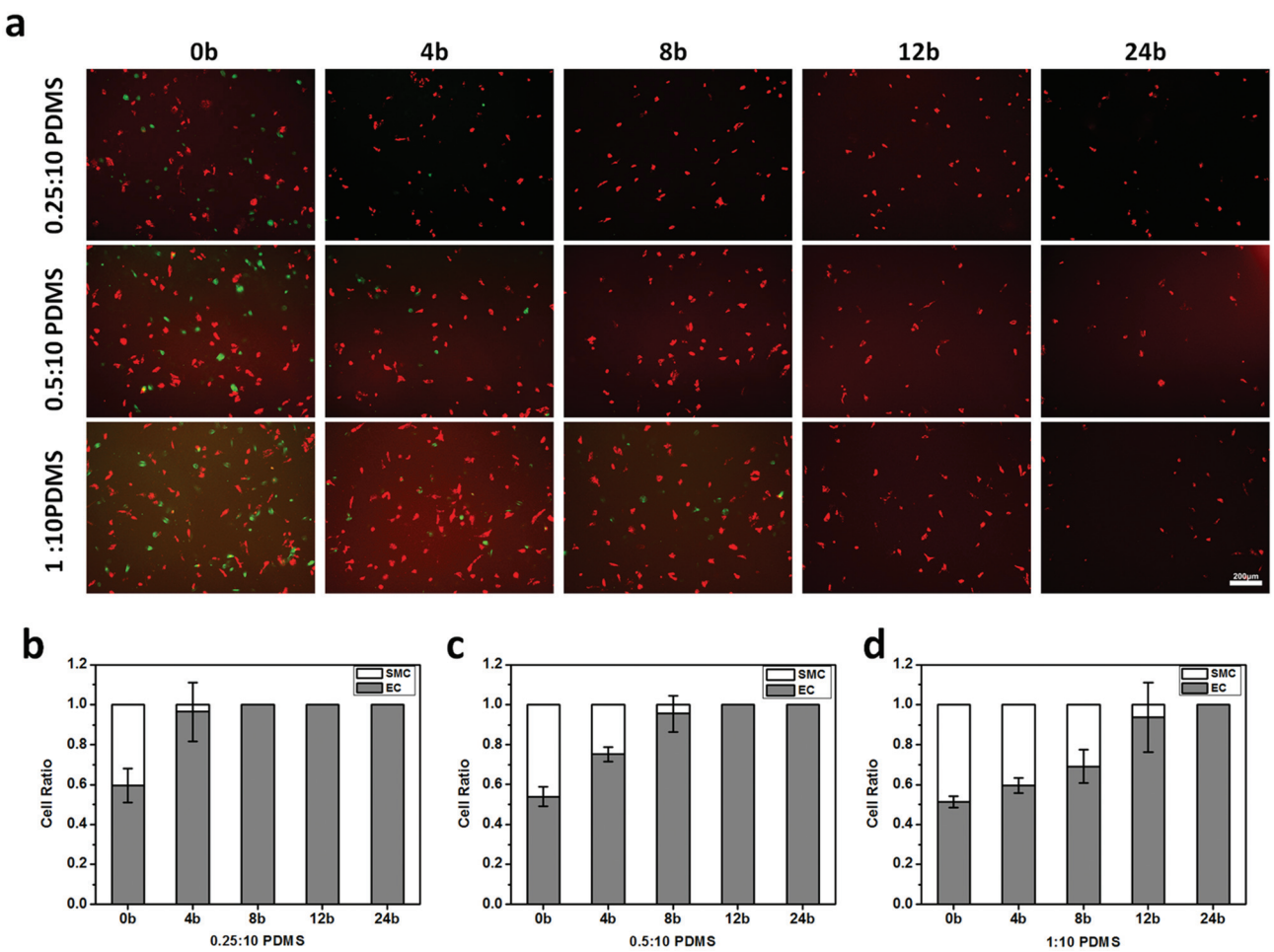

Fig. 8 Selective EC adhesion on the PrS/DNA multilayer films with 0, 4, 8, 12 and 24 bilayers (0b, 4b, 8b, 12b and 24b, respectively) fabricated on PDMS substrates. Immunofluorescence images of ECs (stained using anti-vWf, red) and SMCs (stained using anti-calponin, green) in coculture (a). The cell ratio of EC : SMC in coculture when 0.25 : 10 PDMS (b), 0.5 : 10 PDMS (c) and 1 : 10 PDMS (d) were used as substrates. $N = 5$ parallel samples per group. The data are representative of three independent experiments. The scale bar is 200 μm.

importance for fast re-endothelialization and the inhibition of ISR. The traditional methods of regulating their competitiveness were based on the chemical cues of biomaterials. These methods are relatively efficient, but difficult to manipulate and control in real clinical applications. In contrast, the physical parameters of biomaterials could easily be controlled and realized in industrial areas. Therefore, our study offers a promising alternative based on a pure physical method by combining the LbL technique with the concept of complex stiffness.

Experimental

Preparation of substrates and the PrS/DNA multilayer films

The glass, polyethylene terephthalate (PET) and stainless steel (SS) substrates were cleaned in surfactant solution at 57 °C for 30 min and then rinsed with Milli-Q water. Poly(dimethylsiloxane) (PDMS) substrates of various stiffness were prepared by tuning the cross-linking agent to silicone elastomer base (Dow Corning Sylgard 184) ratio. Herein, cross-linking agent to silicone elastomer base ratios of 0.25 : 10, 0.5 : 10 and 1 : 10 w/w were mixed thoroughly and then transferred into tissue culture plates. After degassing under vacuum for 30 min, the PDMS substrates were cured at 60 °C overnight (10–12 h). The PDMS substrates were exposed to nitrogen plasma for enhancing the surface hydrophilicity for 20 min. Protamine sulfate (PrS) and deoxyribonucleic acid (DNA, fish sperm, sodium salt) were purchased from Sangon Biotech (Shanghai, China). PrS (1 mg mL^{-1}) and DNA (1 mg mL^{-1}) were dissolved in a HEPES-NaCl buffer (20 mM HEPES, 0.15 M NaCl, pH 7.4). The (PrS/DNA) multilayer film was constructed by depositing substrates in a solution of PrS for 10 min. After being rinsed by HEPES solution 3 times (1 min per time), substrates were submerged in the solution of DNA for 10 min. Then substrates were rinsed again as described above. The multilayered films were not dried with nitrogen at the end of the adsorption process. The sequence was repeated until the desired bilayer number was reached. The fabricated films were always kept in HEPES-NaCl solution before characterization.

Characterization of the PrS/DNA multilayer films

All the characterizations of the PrS/DNA multilayer films and PDMS substrates were carried out in aqueous conditions. The buildup process of the PrS/DNA multilayer film was monitored using a commercial quartz crystal microbalance with dissipation (QCM-D) (Qsense, Sweden) at room temperature The gold-coated crystals (QSX 301 quartz crystals, Q-sense) were mounted in a fluid cell with one side exposed to the solution. A measurement of the LbL deposition was initiated by switching the liquid exposed to the resonator. The resonant frequency decrease, ΔF (Hz), was measured for each deposition step. During the monitoring, the films were always exposed to a liquid environment. The thickness of the PrS/DNA multilayer film was analyzed using Q-tools software. The surface morphology was measured using atomic force microscopy (AFM, Bruker, USA). AFM imaging was performed in liquid environment. The mean roughness of the multilayer films was analyzed by using NanoScope Analysis v1.4 software (Bruker).

Young's modulus of the multilayer films' surface and PDMS substrates

The Young's modulus of the multilayer films' surface and PDMS was characterized using a NanoIndenter (Agilent G200). A flat-ended cylindrical punch made of diamond was used to measure Young's modulus in water using the "G-Series XP CSM Flat Punch Complex Modulus" method. The indentation depth was 100 nm. Measurements were obtained at eight different sites for each sample.

Cell culture

Human umbilical vein endothelial cells (ECs) and human umbilical artery smooth muscle cells (SMCs) were freshly isolated from human umbilical veins and arteries as described in previous protocols after the approval by the local medical ethics committee. Both cell types were used for experiments between 3 and 8 passages. The ECs were cultured in serum free medium (SFM, Gibco, USA) supplemented with 10% fetal bovine serum (FBS, Gibco, USA), 20 mg ml^{-1} endothelial cell growth supplement (ECGS, BD Biosciences) and 1% UI ml^{-1} streptomycin–penicillin (S/P, Biochemical-tech, China) in culture dishes at 37 °C and 5% CO_2. The SMCs were cultured in SFM supplemented with 10% FBS and 1% UI ml^{-1} S/P in culture dishes at 37 °C and 5% CO_2. The culture medium was changed every 3 days and culture dishes with 80–90% confluence were used for further cell experiments. For the inhibition assay, both cell types were pretreated with 5 μM Rho-kinase inhibitor Y27632.

Initial adhesion of ECs and SMCs

For the cell adhesion assay, all samples were put in 24-well plates. The culture media for cell adhesion was SFM with 10% FBS. The initial EC and SMC seeding density was 1×10^4 cells cm^{-2} in 24-well plates. After culturing for 4 hours, the cells were fixed in 4% paraformaldehyde in PBS for 15 min and permeabilized in TBS (0.15 M NaCl, 50 mM Tris–HCl, pH 7.4) containing 0.2% Triton X-100 (T8787, Sigma, St. Louis, MO, USA) for 5 min. After rinsing three times with TBS, the slides were blocked with 0.1% bovine serum albumin (BSA, Sigma, St. Louis, MO, USA) in TBS for 1 h. The cells were then incubated with F-actin (1 : 500, rhodamine-phalloidin, Sigma, P1951) in TBS for 30 min. For the focal adhesions, the fixing cells were stained using anti-vinculin (1 : 400, Sigma V9131) in TBS with 0.1% BSA for 1 h and then incubated with Alexa Fluor 488-conjugated goat anti-mouse IgG antibody (1 : 500, A11029, Invitrogen, USA) in TBS with 0.1% BSA for 45 min. All the slides were mounted onto coverslips with antifade reagent (ProLong gold, Invitrogen) and viewed under a fluorescence microscope (Axio-vert 200 M, Zeiss, Germany). The fluorescence images were analyzed with Image J software (v 1.38, NIH, Bethesda).

Adhesion of ECs and SMCs in coculture

ECs and SMCs were mixed together completely in a 1 : 1 ratio and seeded in 24-well plates with a cell density of 1×10^4 cells cm^{-2} (5000 cells for each type of cell). After culturing for 4 hours, the cells were fixed in 4% paraformaldehyde in PBS for 15 min and permeabilized in TBS (0.15 M NaCl, 50 mM Tris–HCl, pH 7.4) containing 0.2% Triton X-100 (T8787, Sigma, St. Louis, MO, USA) for 5 min. After rinsing three times with TBS, the slides were blocked with 0.1% bovine serum albumin (BSA, Sigma, St. Louis, MO, USA) in TBS for 1 h. After being incubated with rabbit anti-human von Willebrand factor monoclonal antibody (1 : 500, anti-vWF, Invitrogen, USA) for ECs and anti-calponin (1 : 500, Invitrogen, USA) for SMCs as primary antibodies, cells on glass coverslips were then immersed in goat anti-rabbit Alexa Fluor 568 (1 : 500, A11011, Invitrogen, USA) and goat anti-mouse Alexa Fluor 488 (1 : 500, A11029, Invitrogen, USA). Finally, all stained coverslips were mounted onto glass slides with antifade reagent for fluorescence microscopy and quantitative analysis using Image J software.

Statistical analysis

All data were expressed as mean ± standard deviation (SD). Statistical significance was assessed with ANOVA and Student's *t* test and a probability value of $p < 0.05$ is considered as statistically significant.

Conclusions

In summary, we have reported a facile and broadly applicable approach to achieve selective cell adhesion of ECs by modulating complex surface stiffness through the LbL assembly technique. Surface stiffness can be easily tuned by controlling multilayer film thickness on the stiff substrate *via* adding or reducing the layer number. For the first time, we have been able to achieve selective EC adhesion exclusively through the use of surface stiffness properties without any combination of bioactive molecules. A key advantage of this approach lies in the combination of the stiffness of both the underlying substrates and LbL multilayer film, which thus makes it facile to tune the surface stiffness of various biomedical devices for enhancement of EC competitiveness. This conceptual framework could be extended to cell selection involving various cell pairs with inherently different properties, such as normal and cancer cells or stem cells before and after differentiation. We believe that this approach provides considerable promise for developing cell-based functional biomaterials.

Acknowledgements

Financial support from the National Natural Science Foundation of China (21174126, 51103126, 51333005, 21374095), China National Funds for Distinguished Young Scientists (51025312), the National Basic Research Program of China (2011CB606203), Open Project of State Key Laboratory of Supramolecular Structure and Materials (SKLSSM201316), Research Fund for the Doctoral Program of Higher Education of China (20110101110037, 20110101120049 and 20120101130013), the Qianjiang Excellence Project of Zhejiang Province (2013R10035), and the International Science & Technology Cooperation Program of China (2014DFG52320) is gratefully acknowledged. We thank Professor Junqi Sun and Yan Wang from the State Key Laboratory of Supramolecular Structure and Materials, College of Chemistry, Jilin University, for their kind help in the measurement of surface stiffness.

Notes and references

1 Z. Reiner, *Curr. Atheroscler. Rep.*, 2014, **16**, 420.
2 A. Tan, Y. Farhatnia, A. de Mel, J. Rajadas, M. S. Alavijeh and A. M. Seifalian, *J. Biotechnol.*, 2013, **164**, 151–170.
3 F. Otsuka, A. V. Finn, S. K. Yazdani, M. Nakano, F. D. Kolodgie and R. Virmani, *Nat. Rev. Cardiol.*, 2012, **9**, 439–453.
4 G. G. Stefanini and D. R. Holmes, *N. Engl. J. Med.*, 2013, **368**, 254–265.
5 A. S. Puranik, E. R. Dawson and N. A. Peppas, *Int. J. Pharm.*, 2013, **441**, 665–679.
6 D. Goh, A. Tan, Y. Farhatnia, J. Rajadas, M. S. Alavijeh and A. M. Seifalian, *Mol. Pharmaceutics*, 2013, **10**, 1279–1298.
7 R. Wessely, *Nat. Rev. Cardiol.*, 2010, **7**, 194–203.
8 L. P. Brewster, E. M. Brey and H. P. Greisler, *Adv. Drug Delivery Rev.*, 2006, **58**, 604–629.
9 J. Hoggatt, K. S. Mohammad, P. Singh and L. M. Pelus, *Blood*, 2013, **122**, 2997–3000.
10 Q. Li, N. Bohin, T. Wen, V. Ng, J. Magee, S. C. Chen, K. Shannon and S. J. Morrison, *Nature*, 2013, **504**, 143–147.
11 O. Herault, K. J. Hope, E. Deneault, M. Trost, N. Mayotte, J. Chagraoui, B. T. Wilhelm, S. Cellot, M. Sauvageau, P. Thibault and G. Sauvageau, *Blood*, 2010, **116**, 670–671.
12 H. Schollnberger, N. Beerenwinkel, R. Hoogenveen and P. Vineis, *Cancer Res.*, 2010, **70**, 6797–6803.
13 J. Garcia-Roman and A. Zentella-Dehesa, *Cancer Lett.*, 2013, **335**, 259–269.
14 Y. Wei, Y. Ji, L. L. Xiao, Q. K. Lin, J. P. Xu, K. F. Ren and J. Ji, *Biomaterials*, 2013, **34**, 2588–2599.
15 H. Chang, K. F. Ren, J. L. Wang, H. Zhang, B. L. Wang, S. M. Zheng, Y. Y. Zhou and J. Ji, *Biomaterials*, 2013, **34**, 3345–3354.
16 S. R. Meyers, P. T. Hamilton, E. B. Walsh, D. J. Kenan and M. W. Grinstaff, *Adv. Mater.*, 2007, **19**, 2492–2498.
17 F. Sharif, S. O. Hynes, K. J. A. McCullagh, S. Ganley, U. Greiser, P. McHugh, J. Crowley, F. Barry and T. O'Brien, *Gene Ther.*, 2012, **19**, 321–328.
18 J. Yang, Y. Zeng, C. Zhang, Y. X. Chen, Z. Y. Yang, Y. J. Li, X. G. Leng, D. L. Kong, X. Q. Wei, H. F. Sun and C. X. Song, *Biomaterials*, 2013, **34**, 1635–1643.
19 Y. Akakabe, M. Koide, Y. Kitamura, K. Matsuo, T. Ueyama, S. Matoba, H. Yamada, K. Miyata, Y. Oike and K. Ikeda, *Nat. Commun.*, 2013, **4**, 13.

20 J. Liu, Y. H. Tan, H. F. Zhang, Y. Zhang, P. W. Xu, J. W. Chen, Y. C. Poh, K. Tang, N. Wang and B. Huang, *Nat. Mater.*, 2012, **11**, 734–741.
21 W. E. Thomas, D. E. Discher and V. P. Shastri, *MRS Bull.*, 2010, **35**, 578–583.
22 A. D. Bershadsky, N. Q. Balaban and B. Geiger, *Annu. Rev. Cell Dev. Biol.*, 2003, **19**, 677–695.
23 J. S. Park, J. S. Chu, A. D. Tsou, R. Diop, Z. Y. Tang, A. J. Wang and S. Li, *Biomaterials*, 2011, **32**, 3921–3930.
24 S. Nemir and J. L. West, *Ann. Biomed. Eng.*, 2010, **38**, 2–20.
25 P. C. Georges, W. J. Miller, D. F. Meaney, E. S. Sawyer and P. A. Janmey, *Biophys. J.*, 2006, **90**, 3012–3018.
26 A. J. Engler, S. Sen, H. L. Sweeney and D. E. Discher, *Cell*, 2006, **126**, 677–689.
27 J. P. Winer, S. Oake and P. A. Janmey, *PLoS One*, 2009, **4**, 11.
28 P. A. Janmey and R. T. Miller, *J. Cell Sci.*, 2011, **124**, 9–18.
29 A. Buxboim, K. Rajagopal, A. E. X. Brown and D. E. Discher, *J. Phys.: Condens. Mater.*, 2010, **22**, 194116.
30 A. Buxboim, I. L. Ivanovska and D. E. Discher, *J. Cell Sci.*, 2010, **123**, 297–308.
31 S. Shimomura, H. Matsuno and K. Tanaka, *Langmuir*, 2013, **29**, 11087–11092.
32 C. H. R. Kuo, J. Xian, J. D. Brenton, K. Franze and E. Sivaniah, *Adv. Mater.*, 2012, **24**, 6059–6064.
33 J. F. Quinn, A. P. R. Johnston, G. K. Such, A. N. Zelikin and F. Caruso, *Chem. Soc. Rev.*, 2007, **36**, 707–718.
34 J. Borges and J. F. Mano, *Chem. Rev.*, 2014, **114**, 8883–8942.
35 G. Decher, *Science*, 1997, **277**, 1232–1237.
36 A. Schneider, G. Francius, R. Obeid, P. Schwinte, J. Hemmerle, B. Frisch, P. Schaaf, J. C. Voegel, B. Senger and C. Picart, *Langmuir*, 2006, **22**, 1193–1200.
37 L. Richert, F. Boulmedais, P. Lavalle, J. Mutterer, E. Ferreux, G. Decher, P. Schaaf, J. C. Voegel and C. Picart, *Biomacromolecules*, 2004, **5**, 284–294.
38 S. W. Lee, K. E. Tettey, I. L. Kim, J. A. Burdick and D. Lee, *Macromolecules*, 2012, **45**, 6120–6126.
39 T. Boudou, T. Crouzier, R. Auzely-Velty, K. Glinel and C. Picart, *Langmuir*, 2009, **25**, 13809–13819.
40 J. Blacklock, A. Vetter, A. Lankenau, D. Oupicky and H. Mohwald, *Biomaterials*, 2010, **31**, 7167–7174.
41 Z. Zhang, Y. X. Lai, L. Yu and J. D. Ding, *Biomaterials*, 2010, **31**, 7873–7882.
42 B. Geiger, J. P. Spatz and A. D. Bershadsky, *Nat. Rev. Mol. Cell Biol.*, 2009, **10**, 21–33.
43 R. H. Liu, X. Y. Chen, S. H. Gellman and K. S. Masters, *J. Am. Chem. Soc.*, 2013, **135**, 16296–16299.
44 J. H. Huang, S. V. Grater, F. Corbellinl, S. Rinck, E. Bock, R. Kemkemer, H. Kessler, J. D. Ding and J. P. Spatz, *Nano Lett.*, 2009, **9**, 1111–1116.
45 W. Chen, L. G. Villa-Diaz, Y. Sun, S. Weng, J. K. Kim, R. H. W. Lam, L. Han, R. Fan, P. H. Krebsbach and J. Fu, *ACS Nano*, 2012, **6**, 4094–4103.
46 R. G. Wells, *Hepatology*, 2008, **47**, 1394–1400.
47 D. E. Discher, P. Janmey and Y. L. Wang, *Science*, 2005, **310**, 1139–1143.
48 V. Gribova, R. Auzely-Velty and C. Picart, *Chem. Mater.*, 2012, **24**, 854–869.
49 K. F. Ren, T. Crouzier, C. Roy and C. Picart, *Adv. Funct. Mater.*, 2008, **18**, 1378–1389.
50 Y. X. Sun, K. F. Ren, J. L. Wang, G. X. Chang and J. Ji, *ACS Appl. Mater. Interfaces*, 2013, **5**, 4597–4602.
51 S. Sen, A. J. Engler and D. E. Discher, *Cell. Mol. Bioeng.*, 2009, **2**, 39–48.
52 J. D. Mih, A. Marinkovic, F. Liu, A. S. Sharif and D. J. Tschumperlin, *J. Cell Sci.*, 2012, **125**, 5974–5983.
53 M. Prager-Khoutorsky, A. Lichtenstein, R. Krishnan, K. Rajendran, A. Mayo, Z. Kam, B. Geiger and A. D. Bershadsky, *Nat. Cell Biol.*, 2011, **13**, 1457–1465.
54 N. Wang, I. M. Tolic-Norrelykke, J. X. Chen, S. M. Mijailovich, J. P. Butler, J. J. Fredberg and D. Stamenovic, *Am. J. Physiol.-Cell Physiol.*, 2002, **282**, C606–C616.
55 M. Y. M. Chiang, Y. Yangben, N. J. Lin, J. L. Zhong and L. Yang, *Biomaterials*, 2013, **34**, 9754–9762.
56 D. H. Zeng, T. Juzkiw, A. T. Read, D. W. H. Chan, M. R. Glucksberg, C. R. Ethier and M. Johnson, *Biomech. Model. Mechanobiol.*, 2010, **9**, 19–33.
57 H. Y. Qiu, Y. Zhu, Z. Sun, J. P. Trzeciakowski, M. Gansner, C. Depre, R. R. G. Resuello, F. F. Natividad, W. C. Hunter, G. M. Genin, E. L. Elson, D. E. Vatner, G. A. Meininger and S. F. Vatner, *Circ. Res.*, 2010, **107**, 615–U117.
58 F. J. Byfield, R. K. Reen, T. P. Shentu, I. Levitan and K. J. Gooch, *J. Biomech.*, 2009, **42**, 1114–1119.
59 K. Katoh, Y. Kano, M. Amano, H. Onishi, K. Kaibuchi and K. Fujiwara, *J. Cell Biol.*, 2001, **153**, 569–583.
60 K. Katoh, Y. Kano and Y. Noda, *J. R. Soc., Interface*, 2011, **8**, 305–311.
61 R. K. Assoian and E. A. Klein, *Trends Cell Biol.*, 2008, **18**, 347–352.
62 S. E. Cross, Y. S. Jin, J. Rao and J. K. Gimzewski, *Nat. Nanotechnol.*, 2007, **2**, 780–783.
63 J. Ji, J. H. Fu, W. Y. Yuan and J. C. Shen, *Biomaterials*, 2005, **26**, 6684–6692.
64 Q. G. Tan, J. Ji, M. A. Barbosa, C. Fonseca and J. C. Shen, *Biomaterials*, 2003, **24**, 4699–4705.
65 A. Yonezu, H. Akimoto, S. Fujisawa and X. Chen, *Mater. Des.*, 2013, **52**, 812–820.
66 N. C. A. Razak, I. M. Inuwa, A. Hassan and S. A. Samsudin, *Compos. Interfaces*, 2013, **20**, 507–515.
67 R. S. O'Connor, X. L. Hao, K. Y. Shen, K. Bashour, T. Akimova, W. W. Hancock, L. C. Kam and M. C. Milone, *J. Immunol.*, 2012, **189**, 1330–1339.
68 X. Q. Brown, K. Ookawa and J. Y. Wong, *Biomaterials*, 2005, **26**, 3123–3129.
69 L. Coultas, K. Chawengsaksophak and J. Rossant, *Nature*, 2005, **438**, 937–945.
70 N. L'Heureux, N. Dusserre, G. Konig, B. Victor, P. Keire, T. N. Wight, N. A. F. Chronos, A. E. Kyles, C. R. Gregory, G. Hoyt, R. C. Robbins and T. N. McAllister, *Nat. Med.*, 2006, **12**, 361–365.

